Chemical Physics Letters 677 (2017) 120–126

Contents lists available at ScienceDirect

Chemical Physics Letters

journal homepage: www.elsevier.com/locate/cplett

Research paper

# Fine-tuning of atomic point charges: Classical simulations of pyridine in different environments

Marina Macchiagodena [a,*], Giordano Mancini [a,b,*], Marco Pagliai [a,1], Gianluca Del Frate [a], Vincenzo Barone [a,b]

[a] Scuola Normale Superiore, Piazza dei Cavalieri 7, 56126 Pisa, Italy
[b] Istituto Nazionale di Fisica Nucleare (INFN) sezione di Pisa, Largo Bruno Pontecorvo 3, 56127 Pisa, Italy

ARTICLE INFO

*Article history:*
Received 9 March 2017
In final form 3 April 2017
Available online 5 April 2017

*Keywords:*
Molecular dynamics
Static dielectric constant
Force fields
Virtual sites
Pyridine
Aqueous solution
Organic liquids
Charge fitting

ABSTRACT

A correct description of electrostatic contributions in force fields for classical simulations is mandatory for an accurate modeling of molecular interactions in pure liquids or solutions. Here, we propose a new protocol for point charge fitting, aimed to take into the proper account different polarization effects due to the environment employing virtual sites and tuning the point charge within the polarizable continuum model framework. The protocol has been validated by means of molecular dynamics simulations on pure pyridine liquid and on pyridine aqueous solution, reproducing a series of experimental observables and providing the information for their correct interpretation at atomic level.



## 1. Introduction

Classical Molecular Dynamics (MD) is a powerful tool, which allows to estimate macroscopic properties from microscopic models [1]. This computational approach has demonstrated to be effective in investigating the structure of organic liquids used as solvents in chemical, biological and technological applications. The reliability of simulations in these studies is related to the availability of an accurate *force field* (FF), which describes the interaction at the atomic and molecular level using a set of functional forms [2] based on a limited number of parameters. These are usually derived from quantum mechanical (QM) calculations of isolated molecules for a selected set of molecular targets and/or tuned in order to reproduce some of physical observables used as references. Despite its key role in describing the solvation ability of a substance, the static dielectric constant remains one of the most difficult bulk properties for classical simulations [3] and is especially sensitive to the electrostatic part of the force field. Since the most widely used FFs still rely on partial atomic charges, several strategies have been employed to determine effective values for these quantities; one of the most adopted approaches relies in optimize their values to reproduce the QM derived electrostatic potential of a molecule [4]. The atomic charges depend strongly on the level of theory used in QM calculations and on the description of solvation effects. In this present study, the electrostatic parameters have been obtained through the Charge Model 5 (CM5) [5] taking into account the bulk solvent effects by means of Conductor-like Polarizable Continuum Model (C-PCM) [6]. This allows one to take into account the different polarization effect of various solvents (here pyridine or water) in tuning the effective atomic charges (as explained in Methods and by Fig. 1).

Furthermore, since the presence of hydrogen bonds (HB) has a remarkable effect on magnitude of the static dielectric constant ($\varepsilon$) [7], a thorough description of intermolecular interactions is necessary. One of the problems in the HB description is its directionality. A possible solution is the use of off-site charges (so-called virtual sites or dummy atoms, VS hereafter) with a fixed position with respect to the generating atom that is meant to model the presence of lone pairs [8,9]. In fact, an improved HB description of pyridine in aqueous solution has been obtained employing VS and adjusting the charges on the carbon atoms directly bound to nitrogen to preserve the molecular dipole moment [9]. However, to develop a model for pyridine able to describe the interactions both in aqueous solution and in pure liquid, the atomic charges

* Corresponding authors at: Scuola Normale Superiore, Piazza dei Cavalieri 7, 56126 Pisa, Italy (M. Macchiagodena and G. Mancini).
*E-mail addresses:* marina.macchiagodena@sns.it (M. Macchiagodena), giordano.mancini@sns.it (G. Mancini).
[1] Present address: Università degli Studi di Firenze, Dipartimento di Chimica "Ugo Schiff", Via della Lastruccia 3, 50019 Sesto Fiorentino (Firenze), Italy.

http://dx.doi.org/10.1016/j.cplett.2017.04.004
0009-2614/

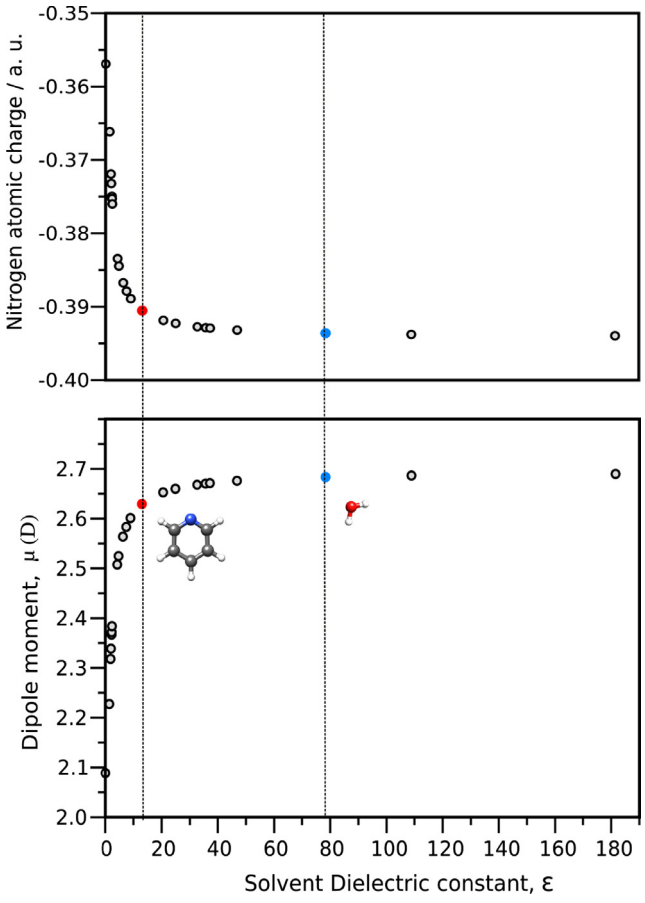


**Fig. 1.** Above: the trend of nitrogen atom partial charge changing the solvent dielectric constant value used in C-PCM. Below: the trend of pyridine molecular dipole moment changing the solvent dielectric constant value used in C-PCM. In red and blue the values obtained imposing pyridine and water as solvents respectively. The nitrogen atomic charges (red and blue circles in the above picture) have been used in our simulations. (For interpretation of the references to colour in this figure legend, the reader is referred to the web version of this article.)

on the whole molecule have been determined with a fitting procedure using as reference parameters both the molecular dipole and quadrupole moments. Therefore, we propose a method for the derivation of partial atomic charges and VS, which completely depends on properties determined at the QM level without any additional empirical parameters. We show that the same strategy works for both pure (liquid) pyridine and its aqueous solution.

The pyridine aqueous solution, as well as the pure liquid, have been studied by means of classical simulations employing several models [9,10,12,13]. Although some of the tested FFs provide reasonable results, here we want to highlight the transferability of our model, able to simulate both pure pyridine and its aqueous solution, overcoming the limitations on these FFs and delivering accurate structural and thermodynamic properties together with the static dielectric constant.

## 2. Methods

Classical MD simulations of both pure liquid and aqueous solution of pyridine were carried out using GROMACS v. 4.6.5 [11] and the OPLS/AA force field [12,13] to describe intramolecular and intermolecular potential with the exception of the pyridine atomic charges, which were estimated using the CM5 population analysis [5]. Density Functional Theory (DFT) calculations were performed at the B3LYP/6-31+G(d) level of theory using GAUSSIAN-09 [14] package and taking into account bulk solvent effects by means of the Conductor-like Polarizable Continuum Model (C-PCM) [6] setting the reference solvent (pyridine or water) and imposing the value of the scaling factor for the sphere radius ($\alpha$) to 1.05. In Fig. 1, the nitrogen atom charge, and the pyridine dipole moment, are reported to show the polarization effects induced by several solvents with increasing dielectric constant (from 1.43 to 181.96) and implicitly described by the C-PCM. A virtual site (VS) was located at the position of the centroid of the localized molecular orbital describing the $sp^2$ lone-pair of the nitrogen atom using the Pipek-Mezey localization procedure [15] (the centroid distance from the nitrogen atom has been constrained during the simulation). The charge on the VS has been obtained adjusting the atomic charges of pyridine through a fitting procedure to reproduce the calculated dipole and quadrupole moments, as indicated in Table 1 (for atom labeling Table 1).

The simulation for the pyridine pure liquid was performed on a system containing 500 molecules, whereas the simulation of the aqueous solutions was performed on one pyridine and 512 TIP3P-FB [16] water molecules. In both cases, we employed a cubic box with periodic boundary conditions. After a steepest descent energy minimization the systems were heated up to 298.15 K for 200 ps (using the velocity-rescale [17] thermostat and $\tau = 0.1$ ps) and then the time step and temperature coupling constant were increased to 2.0 fs and 0.2 ps respectively, and systems were let to converge to uniform density in a NPT ensemble (using the Parrinello-Rahman barostat [18] and $\tau = 0.1$ ps).

Afterward production runs were run in the NVT ensemble [17], fixing the fastest degrees of freedom with LINCS algorithm ($\delta t = 2.0$ fs) [19]. The total sampling time was 50 ns for both the pure liquid and the aqueous solution. Electrostatic interactions were evaluated using the particle-mesh Ewald (PME) [20] method with a grid spacing of 1.2 Å and a spline interpolation of order 4.

Harder et al. [21] have proposed an OPLS3 pyridine model, which also has an off-site charge on the nitrogen atom and reproduces well the hydration free energy (−4.3 kcal/mol). We performed a MD simulation using this force field, to determine structural information on pure liquid and compare the obtained results with our model. The main difference between OPLS3 and our model is the charge on nitrogen atom, which is not null in OPLS3 (+0.179 e) and the procedure employed to define the virtual site position [8]. An *ab initio* molecular dynamics (AIMD) simulation of a pyridine aqueous solution at ambient temperature was carried out using the CP2K program [22,23] to further assess the reliability of our procedure to describe the hydrogen bond interactions and their directional character. We considered a cubic box of size 11.77 Å containing 1 pyridine and 50 water molecules and subjected to periodic boundary conditions. We performed a simulation of 20 ps in the NVE ensemble with a time step of 0.1 fs. The electronic structure was calculated with DFT, utilizing the BLYP functional [24,25]. The TZV2P basis set was used in conjunction with the GTH pseudopotentials [26,27]. A plane wave cutoff of 340 Ry was adopted for electron density. Van der Waals interactions have been described by the method proposed by Grimme [28].

Dielectric constant and density have been evaluated using standard tools provided with GROMACS. To calculate the heat of vaporization, $\Delta H_{vap}$, gas-phase simulations of 2 ns ($\delta t = 0.2$ fs) have been added for both systems. The $\Delta G_{hyd}$ were calculated using Bennett acceptance ratio (BAR), [29] a free energy perturbation (FEP) method, performing the simulations with GROMACS v. 4.6.5. Structural analysis was performed with TRAVIS package [30]. Spatial distribution function (sdf) graphs were prepared using the Caffeine [31] molecular viewer.

The relative orientation of first neighbour pyridine molecules was also investigated by means of the KMeans clustering algorithm

**Table 1**
The CM5 charges (e) for pyridine calculated at the B3LYP/6-31+G(d) level and used in the simulations (adjusted) taking into account the solvent (pyridine or water) effect by means of C-PCM. In the column Δ(CM5-Adj) is reported the difference between the calculated and used charges. The molecular dipole (μ) and quadrupole (Q) moments obtained from CM5 charges and employed during the fitting procedure in presence of VS are also reported. In the last row, the pyridine and water atoms labeling and the virtual site position are indicated.

| | q (e) | | | | | |
|---|---|---|---|---|---|---|
| | Solvent = pyridine | | | Solvent = water | | |
| | CM5 | Adjusted | Δ (CM5-Adj) | CM5 | Adjusted | Δ (CM5-Adj) |
| C1-C2 | 0.035648 | 0.001047 | 0.034601 | 0.034855 | −0.000150 | 0.035005 |
| C3-C4 | −0.090393 | −0.113328 | 0.022935 | −0.089909 | −0.113072 | 0.023163 |
| C5 | −0.068839 | −0.113375 | 0.044536 | −0.068037 | −0.113058 | 0.045021 |
| N | −0.390529 | 0.000000 | −0.390529 | −0.393605 | 0.000000 | −0.393605 |
| VS | 0.000000 | −0.329297 | 0.329297 | 0.000000 | −0.331658 | 0.331658 |
| H1-H2 | 0.112816 | 0.151052 | −0.038236 | 0.112965 | 0.151590 | −0.038625 |
| H3-H4 | 0.113452 | 0.095364 | 0.018088 | 0.114284 | 0.096017 | 0.018267 |
| H5 | 0.116322 | 0.174402 | −0.058080 | 0.117252 | 0.175946 | −0.058694 |
| μ (D) | −2.62941 | | | −2.68354 | | |
| Q(XX) (D•Å) | −2.15265 | | | −2.15585 | | |
| Q(YY) (D•Å) | 7.75545 | | | 7.78872 | | |
| Q(ZZ) (D•Å) | −5.60280 | | | −5.63287 | | |

Pyridine and water atoms labeling. Virtual site position

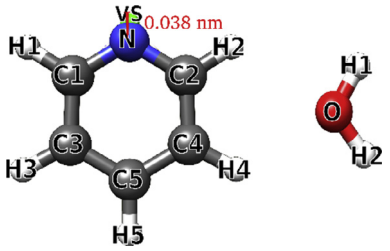


[32] using the Scikit-learn library [33]; the optimal number of clusters was determined with the Calinski-Harabasz criterion [34].

## 3. Results

### 3.1. Aqueous solution

The structure of pyridine in aqueous solution is characterized by the hydrogen bond interaction between the nitrogen atom of the heterocyclic ring and a hydrogen atom of the solvent molecules (Fig. 2a). The oxygen atom also interacts with the hydrogen atoms of pyridine, leading to a weaker interaction, as confirmed by a longer interatomic distance (see Fig. 2a). In fact, the first maximum in $g_{N\cdots H}(r)$ and $g_{CH\cdots O}(r)$ radial distribution functions (rdf) occurs around 1.8 Å and 3.2 Å respectively. The relative sdf of water hydrogen and oxygen atoms around the pyridine are reported in Fig. 2b, corroborating the presence of a hydrogen bond between the nitrogen and the hydrogen atoms. The isovalue adopted to show the results does not lead to similar isosurfaces involving the pyridine hydrogen atoms, confirming the weaker character of the interaction with solvent. The oxygen atom density is localized above and below the aromatic ring suggesting the presence of a HB$\cdots\pi$ interactions. In fact, the radial distribution function between the pyridine ring center (RC) and the oxygen atom (red line in Fig. 2a) confirms the presence of such an interaction. To demonstrate the usefulness of VS to mimic the lone pair of the $sp^2$ nitrogen atom, in Fig. 2c are also shown the same sdf obtained analyzing the simulations of our model when the VS is removed. In this case the simulation was performed using the CM5 charges (Table 1) without the VS and the HB density distribution shows a lack in directionality, the sdf is not localized in the ring plane but above and below it.

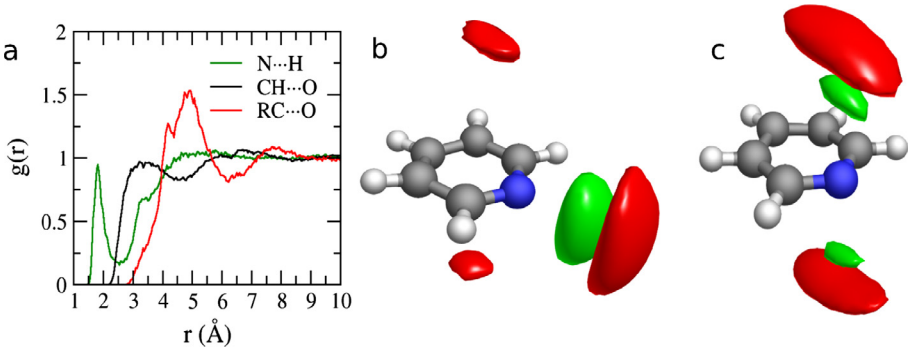


**Fig. 2.** a. Radial distribution functions between the pyridine nitrogen (green) and hydrogen (black) atoms and the water hydrogen and oxygen atoms respectively. In red the g (r) between the pyridine ring center (RC) and the oxygen atom of water. b. Isosurface, obtained from MD simulation, of water oxygen (red), hydrogen atoms (green) around the pyridine molecule at an isovalue of 68 and 60 $nm^{-3}$ respectively. c. Isosurface of water oxygen (red), hydrogen atoms (green) around the pyridine molecule at an isovalue of 68 and 60 $nm^{-3}$ respectively. The results are obtained with our model deprived of VS. (For interpretation of the references to colour in this figure legend, the reader is referred to the web version of this article.)

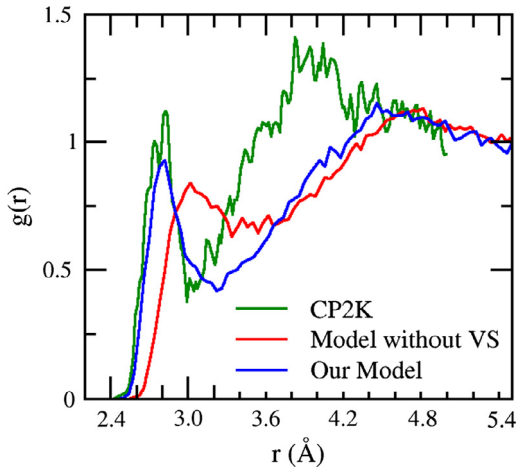


**Fig. 3.** Radial distribution functions between the pyridine nitrogen and the water oxygen ($g_{N\cdots O}(r)$) atoms obtained from three simulations: our (blue), CP2K (green) and our model without the virtual site (red). (For interpretation of the references to colour in this figure legend, the reader is referred to the web version of this article.)

As described in Section 2, we also performed an *ab initio* simulation for purposes of comparison. Therefore, in Fig. 3 we reported the rdf between the pyridine nitrogen atom and the water oxygen atom obtained from three simulation: our force field, CP2K and a simulation performed without VS. The comparison between CP2K and our model (with VS) is remarkable and confirms the usefulness of VS to describe the hydrogen bond.

### 3.2. Pure pyridine

A first structural analysis of pure pyridine is reported in Fig. 4a, where the rdf between nitrogen atoms is shown. The $g_{N\cdots N}(r)$ shows two distinct peaks, one around 4.9 Å and one around 5.9 Å. A similar rdf was obtained by Jorgensen and McDonald [35] and by Baker and Grant [36], who have previously studied liquid pyridine using the OPLS and OPLS-CS force fields respectively. Jorgensen and McDonald attributed the first peak to antiparallel contacts and the second to dimers that are offset stacked with parallel (head-to-tail) dipoles. According to Baker and Grant, the first peak results from a structure in which a pyridine molecule donates a hydrogen bond through the H1/H2 hydrogen atoms (for atom

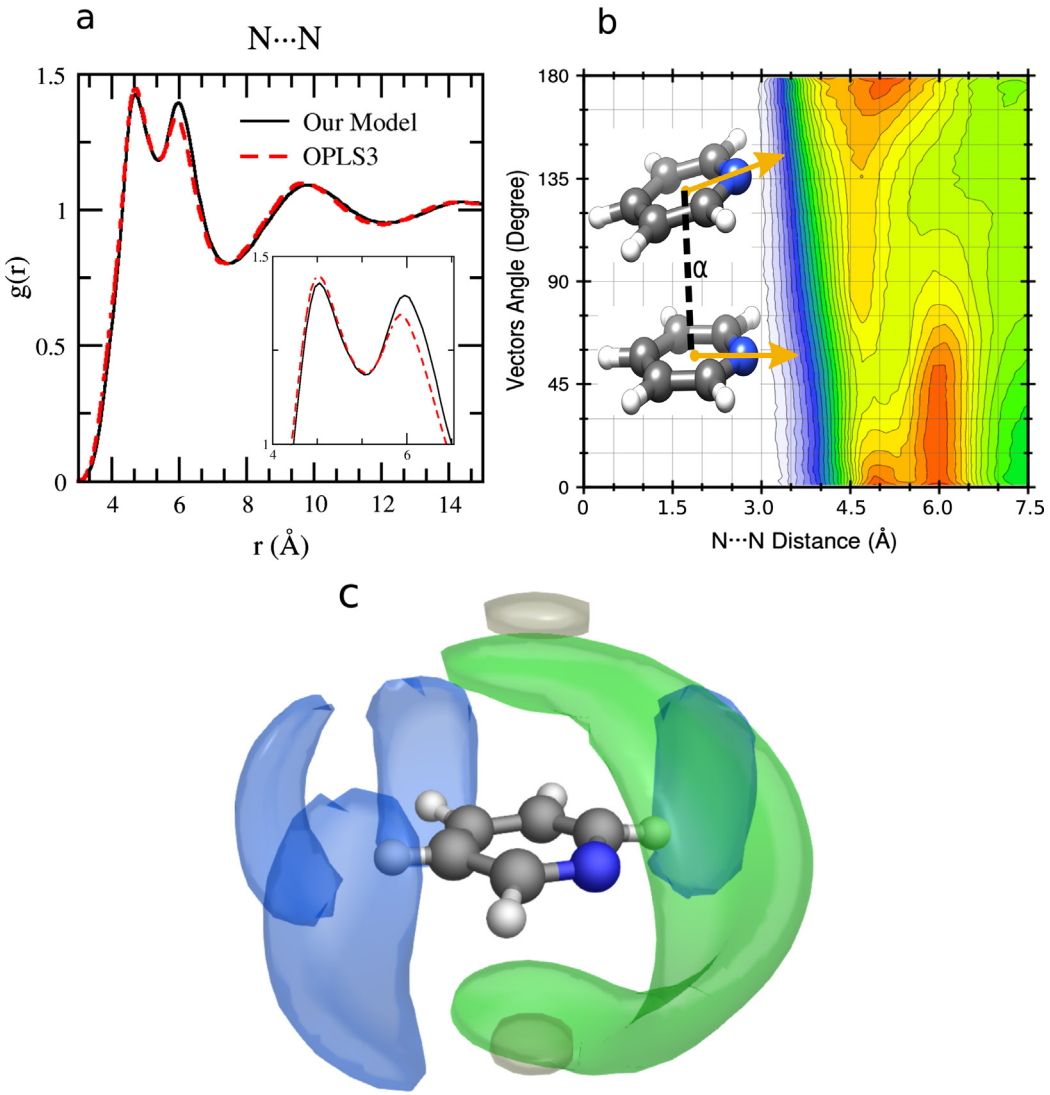


**Fig. 4.** a. Radial distribution function between N···N in pure liquid (black: our model; red: OPLS3). b. Combined distribution function between N···N distance and the angle α formed between the vectors connecting the center of the ring and the nitrogen atom (orange vectors in picture b). c. Isosurface of the pyridine nitrogen atom (blue), carbon atoms (gray) and hydrogen atoms (green) around the pyridine molecule at an isovalue of 15, 14 and 11 $nm^{-3}$ respectively. The results are obtained from the pure liquid pyridine simulation. (For interpretation of the references to colour in this figure legend, the reader is referred to the web version of this article.)

labeling see Table 1) and the second peak from one in which a pyridine molecule donates a hydrogen bond using the H3/H4 hydrogen atoms. Interpretation of the peaks in structural terms can be obtained by computing the combined distribution function (cdf) between the N···N distance and the angle formed between the vectors connecting pyridine ring center and nitrogen atom. The cdf is shown in Fig. 4b and permits to attribute the first peak to an antiparallel arrangement and the second to a parallel arrangement and to an interaction, which occurs between rings forming an angle up to 45°. To better understand the relative orientation of pyridine molecules we applied KMeans [32] selecting as clustering features the first neighbour distances between the center of rings, the nitrogen and the C5 atoms; by inspection of Fig. 4, we determined an 8.0 Å cut-off for each feature. Application of the Calinski-Harabasz score [34] indicated the optimal number of clusters at NC = 2 containing 56% and 44% of data points, respectively. The first neighbour distances of the cluster centers show an approximately parallel orientation of molecules. The N···N and C5···C5 distances for the two cluster centers are of 5.78, 5.53 and 6.68, 6.87 Å, respectively. This corresponds to the arrangements where the angle between two rings is 0° or around 45° (see insert in Fig. 4b).

In Fig. 4a we also reported the $g_{N\cdots N}(r)$ calculated from the OPLS3 simulation, which shows a slightly lower peak at around 5.9 Å suggesting that in our case the parallel arrangement is more abundant. This observation will be useful to evaluate the differences between the calculated bulk properties.

The average densities of nitrogen, carbon and hydrogen atoms around the molecules are reported in Fig. 4c. The hydrogen atoms density around nitrogen atom supports the hypothesis that the interactions in the pyridine liquid are dominates by N···HC hydrogen bonds. The same is true for the nitrogen atom density, localized near hydrogen atoms. This spatial distribution function deserves an additional consideration: the density does not point along the C—H bond but is localized in the center of two C—H bonds; this is due to the possibility of having simultaneous interactions between the nitrogen atom and two hydrogen atoms. Furthermore, the localization of hydrogen atoms (as well as the carbon) density above and below the aromatic ring, suggests that the arrangements are stabilized by the formation of CH···π interactions. It is also noteworthy that the N···HC interactions mainly involve, as expected, the H3, H4 and H5 hydrogens.

Fig. 5a sketches the cdf between two different N···H distances; this analysis confirms the simultaneous interaction in the pure liquid, as already shown by the sdf of Fig. 4c. Fig. 5b shows also the relative cdf for the water solution between two N···H(water) distances; it is apparent that the interaction involves only one hydrogen atom and confirms the results of sdf analysis. Fig. 5a-b reports also the single rdf, which points out a stronger interaction in the pyridine aqueous solution (shorter distance N···H involved) with respect to the pure liquid (higher maximum in the radial distribution function).

In the following, we discuss results obtained for bulk properties (Table 2). A correct reproduction of the static dielectric constant of the pure liquid is particularly important in view of the large use of pyridine as solvent for several processes of technological relevance [37]. Our pure liquid model, using CM5 charges (C-PCM) and a VS for $sp^2$ nitrogen atom, allows one to obtain a dielectric constant value of 11.2 ± 0.2 in good agreement with the experimental value of 12.4 [37]. This result represents a non-negligible improvement with respect of the value of 6.7 ± 0.1 obtained using the standard OPLS force field [3]. Furthermore, the analysis of a MD simulation on pure pyridine performed in the present study employing the OPLS3 force field [21] leads to less accurate values of both static dielectric constant (9.1 ± 0.2) and density (1008.9 ± 0.2 kg/m$^3$). Looking at Fig. 4a, the better value of dielectric constant could be due to a higher number of parallel pyridine or nearly parallel pyridine molecules issuing from our force field. In Fig. 6 we reported the rdf between the nitrogen and the hydrogen atoms of pyridine: our model has a higher peak for the $g_{N\cdots H5}(r)$ which is in agreement with the parallel orientation of pyridine molecule.

Other properties, often used to validate a FF, such as density and heats of vaporization ($\Delta H_{vap}$), were also calculated and their computed values are in agreement with the experimental results.

**Table 2**
Computed values and experimental data for static dielectric constant, density (kg/m$^3$), heat of vaporization (kcal/mol) and free energy of hydration (kcal/mol) for pyridine molecule.

| Properties | This work | EXP |
|---|---|---|
| ε | 11.2 ± 0.2 | 12.4 [38] |
| ρ (kg/m$^3$) | 995.3 ± 0.2 | 977.8 [39] |
| $\Delta H_{vap}$ (kcal/mol) | 10.7 ± 0.2 | 9.61 [39] |
| $\Delta G_{hyd}$ (kcal/mol) | −4.23 ± 0.02 | −4.7 [21] |

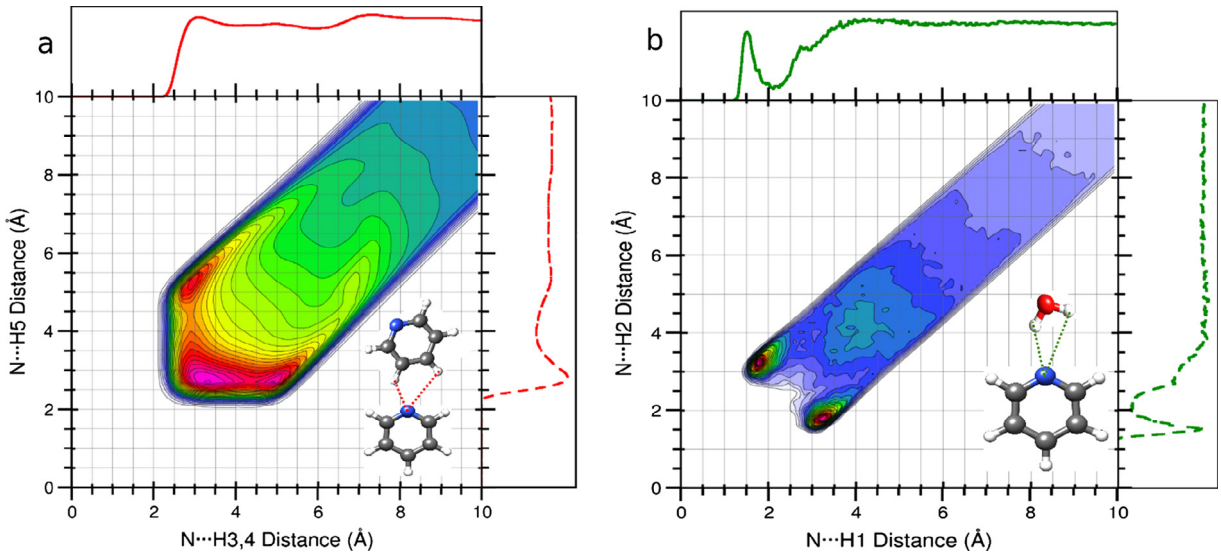


**Fig. 5.** a. Combined distribution function between N···H3,4 e N···H5, like indicated in insert, obtained from the pure pyridine liquid simulation. b. Combined distribution function between N···H1 and N···H2 obtained from the water pyridine solution.

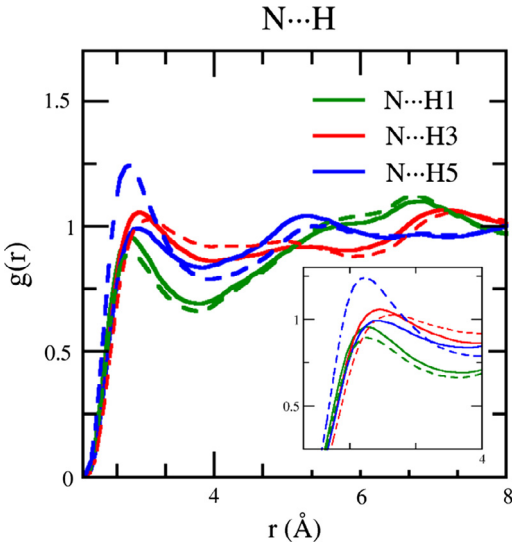


**Fig. 6.** Radial distribution function between N and H1 (green), H3 (red), H5 (blue) hydrogen atoms. In continuous line OPLS3, in dashed line our model. (For interpretation of the references to colour in this figure legend, the reader is referred to the web version of this article.)

We obtained a density value of 995.3 ± 0.2 kg/m$^3$ (the experimental value is of 977.8 kg/m$^3$ [39]); instead, the calculated $\Delta H_{vap}$ value is equal to 10.7 ± 0.2 kcal/mol. Since the experimental value is 9.61 kcal/mol [39] and OPLS provides a value of 9.76 kcal/mol [40], in this case OPLS performs better than our model.

Furthermore, the availability of the pyridine aqueous simulation, allows us to derive the free energy of hydration, $\Delta G_{hyd}$. The result obtained is of −4.23 kcal/mol (Table 2) with an error around the 10% with respect to the experimental value of −4.7 kcal/mol [20].

## 4. Conclusions

In this study, we have presented an improved force field of pyridine, which allows one to describe both the pure liquid and the aqueous solution. The main feature of the new force field is the use of partial atomic charges that takes into account in an effective way the polarization effects of the environment, without adding any *ad hoc* correction term to the FF. By changing the dielectric constant value in the C-PCM protocol, we have the possibility of describing by the same model the pyridine aqueous solution and the pure pyridine liquid. Furthermore, since the hydrogen bonds have been found to be important in describing the structure, we introduce a virtual site (VS) to mimic the lone pair of the sp$^2$ nitrogen atom. The VS allows one to describe the directional character of hydrogen bond interaction in agreement with reference *ab initio* molecular dynamics simulation, without compromising the description of the pure liquid. In fact, the VS can describe both the interaction involving only a couple of atoms (pyridine-water) and a simultaneous interaction involving more than two atoms, like the interaction found in pure pyridine liquid, which may involve the nitrogen atom of one pyridine molecule and two hydrogen atoms of another.

Starting from these satisfactory structural results, we computed also thermodynamic properties for the pure liquid. We were able to reproduce the static dielectric constant, which is often poorly reproduced with standard FFs. Although usually not included in FF validation, the dielectric constant represents a very important parameter governing the solvation capacity. At the same time, satisfactory results were obtained for density and vaporization enthalpy.

## Acknowledgments

The authors thank Prof. Gianni Cardini for useful discussions and the SMART Lab technical staff for managing the computing facilities at SNS. MM thanks the support of Scuola Normale Superiore grant "Giovani Ricercatori 2015". The research leading to these results has received funding from the European Research Council under the European Union's Seventh Framework Programme (FP/2007-2013)/ERC Grant Agreement n. [320951].

## References

[1] D.C. Rapaport, The art of molecular dynamics simulation, 2nd ed., Cambridge University Press, Cambridge; UK, New York, NY, 2004.
[2] A.R. Leach, Molecular modelling principles and applications, 2nd ed., Prentice Hall, Harlow, England; New York, 2001.
[3] C. Caleman, P.J. van Maaren, M. Hong, J.S. Hub, L.T. Costa, D. van der Spoel, Force field benchmark of organic liquids: density, enthalpy of vaporization, heat capacities, surface tension, isothermal compressibility, volumetric expansion coefficient, and dielectric constant, J. Chem. Theory Comp. 8 (1) (2012) 61–74.
[4] C.I. Bayly, P. Cieplak, W. Cornell, P.A. Kollman, A well-behaved electrostatic potential based method using charge restraints for deriving atomic charges: the RESP model, J. Phys. Chem. 97 (40) (1993) 10269–10280.
[5] A.V. Marenich, S.V. Jerome, C.J. Cramer, D.G. Truhlar, Charge Model 5: an extension of Hirshfeld population analysis for the accurate description of molecular interactions in gaseous and condensed phases, J. Chem. Theory Comput. 8 (2) (2012) 527–541.
[6] V. Barone, M. Cossi, Quantum calculation of molecular energies and energy gradients in solution by a conductor solvent model, J. Phys. Chem. 102 (11) (1998) 1995–2001.
[7] S. Goldman, C. Joslin, Why hydrogen-bonded liquids tend to have high static dielectric constants, J. Phys. Chem. 97 (47) (1993) 12349–12355.
[8] M. Macchiagodena, G. Mancini, M. Pagliai, V. Barone, Accurate prediction of bulk properties in hydrogen bonded liquids: amides as case studies, Phys. Chem. Chem. Phys. 18 (2016) 25342–25354.
[9] M. Pagliai, G. Mancini, I. Carnimeo, N. De Mitri, V. Barone, Electronic absorption spectra of pyridine and nicotine in aqueous solution with a combined molecular dynamics and polarizable QM/MM approach, J. Comput. Chem. 38 (2017) 319–335.
[10] I. Cacelli, A. Cimoli, P.R. Livotto, G. Prampolini, An automated approach for the parameterization of accurate intermolecular force-fields: pyridine as a case study, J. Comput. Chem. 33 (2012) 1055–1067.
[11] B. Hess, C. Kutzner, D. van der Spoel, E. Lindahl, GROMACS 4: algorithms for highly efficient, load-balanced, and scalable molecular simulation, J. Chem. Theory Comput. 4 (3) (2008) 435–447.
[12] W.L. Jorgensen, D.S. Maxwell, J. Tirado-Rives, Development and testing of the OPLS all-atom force field on conformational energetics and properties of organic liquids, J. Am. Chem. Soc. 118 (45) (1996) 11225–11236.
[13] W.L. Jorgensen, J. Tirado-Rives, Potential energy functions for atomic-level simulations of water and organic and biomolecular systems, Proc. Natl. Acad. Sci. USA 102 (18) (2005) 6665–6670.
[14] M.J. Frisch, G.W. Trucks, H.B. Schlegel, G.E. Scuseria, M.A. Robb, J.R. Cheeseman, G. Scalmani, V. Barone, B. Mennucci, G.A. Petersson, H. Nakatsuji, M. Caricato, X. Li, H.P. Hratchian, A.F. Izmaylov, J. Bloino, G. Zheng, J.L. Sonnenberg, M. Hada, M. Ehara, K. Toyota, R. Fukuda, J. Hasegawa, M. Ishida, T. Nakajima, Y. Honda, O. Kitao, H. Nakai, T. Vreven, J.A. Montgomery, Jr., J.E. Peralta, F. Ogliaro, M. Bearpark, J.J. Heyd, E. Brothers, K.N. Kudin, V. N. Staroverov, R. Kobayashi, J. Normand, K. Raghavachari, A. Rendell, J.C. Burant, S.S. Iyengar, J. Tomasi, M. Cossi, N. Rega, J.M. Millam, M. Klene, J.E. Knox, J.B. Cross, V. Bakken, C. Adamo, J. Jaramillo, R. Gomperts, R.E. Stratmann, O. Yazyev, A.J. Austin, R. Cammi, C. Pomelli, J.W. Ochterski, R.L. Martin, K. Morokuma, V.G. Zakrzewski, G.A. Voth, P. Salvador, J.J. Dannenberg, S. Dapprich, A.D. Daniels, O. Farkas, J.B. Foresman, J.V. Ortiz, J. Cioslowski, D.J. Fox, Gaussian 09 Revision E.01.
[15] J. Pipek, P.G. Mezey, A fast intrinsic localization procedure applicable for ab initio and semiempirical linear combination of atomic orbital wave functions, J. Chem. Phys. 90 (9) (1989) 4916–4926.
[16] L.P. Wang, T.J. Martinez, V.S. Pande, Building force fields an automatic systematic and reproducible approach, J. Phys. Chem. Lett. 5 (2014) 1885–1891.
[17] G. Bussi, D. Donadio, M. Parrinello, Canonical sampling through velocity rescaling, J. Chem. Phys. 126 (1) (2007) 14101.
[18] M. Parrinello, A. Rahman, Strain fluctuations and elastic constants, J. Chem. Phys. 76 (1982) 2662–2666.
[19] B. Hess, H. Bekker, H.J.C. Berendsen, J.G.E.M. Fraaije, LINCS: a linear constraint solver for molecular simulations, J. Comput. Chem. 18 (12) (1997) 1463–1472.
[20] T. Darden, D. York, L. Pedersen, Particle mesh Ewald: an N·log(N) method for Ewald sums in large systems, J. Chem. Phys. 98 (12) (1993) 10089.
[21] E. Harder, W. Damm, J. Maple, C. Wu, M. Reboul, J.Y. Xiang, L. Wang, D. Lupyan, M.K. Dahlgren, J.L. Knight, J.W. Kaus, D.S. Cerutti, G. Krilov, W.L. Jorgensen, R. Abel, R.A. Friesner, OPLS3 a force field providing broad coverage of drug-like small molecules and proteins, J. Chem. Theory Comput. 12 (2016) 281–296.

[22] J. Hutter, M. Iannuzzi, F. Schiffmann, J. VandeVondele, CP2K: atomistic simulations of condensed matter systems, WIREs Comput. Mol. Sci. 4 (1) (2014) 15–25.
[23] CP2K: Open Source Molecular Dynamics. <http://www.cp2k.org>.
[24] A.D. Becke, Density-functional exchange-energy approximation with correct asymptotic behavior, Phys. Rev. A 38 (6) (1998) 3098–3100.
[25] C. Lee, W. Yang, R.G. Parr, Development of the Colle-Salvetti correlation-energy formula into a functional of the electron density, Phys. Rev. 37 (2) (1988) 785–789.
[26] S. Goedecker, M. Teter, J. Hutter, Separable dual-space Gaussian pseudopotentials, Phys. Rev. B 54 (3) (1996) 1703–1710.
[27] C. Hartwigsen, S. Goedecker, J. Hutter, Separable dual-space Gaussian pseudopotentials from H to Rn, Phys. Rev. B 58 (7) (1998) 3641–3662.
[28] S. Grimme, J. Antony, S. Ehrlich, H. Krieg, A consistent and accurate ab initio parametrization of density functional dispersion correction (DFT-D) for the 94 elements H-Pu, J. Chem. Phys. 132 (2010) 154104.
[29] H.C. Bennett, Efficient estimation of free energy differences from Monte Carlo data, J. Comput. Phys. 22 (2) (1976) 245–268.
[30] M. Brehm, B. Kirchner, TRAVIS - a free analyzer and visualizer for Monte Carlo and molecular dynamics trajectories, J. Chem. Inf. Model. 51 (8) (2011) 2007–2023.
[31] A. Salvadori, G. Del Frate, M. Pagliai, G. Mancini, V. Barone, Immersive virtual reality in computational chemistry: applications to the analysis of QM and MM data, Int. J. Quantum Chem. 116 (22) (2016) 1731–1746.
[32] J.B. MacQueen, Some methods for classification and analysis of multivariate observations, Proceedings of 5-th Berkeley Symposium on Mathematical Statistics and Probability, vol. 1, University of California Press, Berkeley, 1967, pp. 281–297.
[33] F. Pedregosa, G. Varoquaux, A. Gramfort, V. Michel, B. Thirion, O. Grisel, M. Blondel, P. Prettenhofer, R. Weiss, V. Dubourg, J. Vanderplas, A. Passos, D. Cournapeau, M. Brucher, M. Perrot, E. Duchesnay, Scikit-learn: machine learning in python, J. Mach. Learn. Res. 12 (2011) 2825–2830.
[34] T. Calinski, J. Harabasz, A dendrite method for cluster analysis, Commun. Stat. - Theory Meth. 3 (1974) 1–27.
[35] W.L. Jorgensen, N.A. McDonald, Development of an all-atom force field for heterocycles properties of liquid pyridine and diazenes, J. Mol. Struct. Theochem. 424 (1–2) (1998) 145–155.
[36] C.M. Baker, G.H. Grant, Modeling aromatic liquids: toluene, phenol, and pyridine, J. Chem. Theory Comput. 3 (2) (2007) 530–548.
[37] E.F.V. Scriven, R. Murugan, Pyridine and pyridine derivatives, Kirk-Othmer Encyclopedia of Chemical Technology, vol. 20, John Wiley & Sons Inc, 2005, pp. 1–53.
[38] E. Lide, Handbook of Chemistry and Physics: A Ready-reference Book of Chemical and Physical Data, Handbook of Chemistry and Physics; CRC Press, Boca Raton, Florida, 1993.
[39] Y. Marcus, The properties of solvents, in: Wiley Series in Solution Chemistry, Wiley, Chichester; New York, 1998.
[40] L.S. Dodda, J.Z. Vilseck, K.J. Cutrona, W.L. Jorgensen, Evaluation of CM5 charges for nonaqueous condensed-phase modeling, J. Chem. Theory Comput. 11 (9) (2015) 4273–4282.